# Influence of Internal Friction on Transport Properties in Sheared Granular Flows

**Shu-San Hsiau, Jr-Yuan Shiu, and Wen-Lung Yang**
Dept. of Mechanical Engineering, National Central University, Chung-Li, 32054 Taiwan, ROC

**Li-Shin Lu**
Dept. of Mechanical Engineering, Northern Taiwan Institute of Science and Technology, Taipei, 11202 Taiwan, ROC

*DOI 10.1002/aic.10977*
*Published online September 1, 2006 in Wiley InterScience (www.interscience.wiley.com).*

*The effect has been studied of the internal friction coefficient of particles on transport properties of sheared granular flows. Experiments were performed in shear cell devices under four different internal friction coefficients of the particles and five different solid fractions. The motions of the granular materials were recorded by a high-speed camera. By using image processing technology and the particle tracking method, we measured and analyzed the distributions of the average velocity, fluctuation velocity, and particle self-diffusion coefficient. Three bi-directional stress gages were used to measure the normal and shear stresses along the upper boundary. According to the experimental results, the stresses and the self-diffusion coefficients of the particles were inverse proportional to the internal friction coefficients. In the same conditions, the normal stresses were apparently higher than the shear stresses. The fluctuation and the self-diffusion coefficients in the streamwise direction were obviously higher than those in the transverse direction. The normal and shear stresses were found to increase with the solid fraction, but the diffusion coefficients were greater in a more dilute flow system. In addition, the deviations of self-diffusion coefficients in the low solid fraction condition were much greater than those in the high solid fraction condition.* © 2006 American Institute of Chemical Engineers *AIChE J,* 52: 3592–3599, 2006

*Keywords: granular flow, shear cell, internal friction coefficient, stress gage, self-diffusion coefficient*

## Introduction

The dominant mechanism affecting the flow behavior of granular materials is the random motions of particles resulting from the interactive collisions between particles.[1] Because the random motions of particles in a granular flow are analogous to the motion of molecules in a gas, the dense-gas kinetic theory[2-4] and molecular dynamic simulation[5] are used to analyze and model the granular flow behavior. One main difference between a granular material system and a molecular system is that the molecules are frictionless and inelastic, but the granules have energy dissipation due to the friction and inelasticity. In fact, the restitution coefficient and friction coefficient are very important properties to particle collisions and play significant roles in the behaviors of the sheared granular flow.

In the dense-gas kinetic theory applied to a granular system, the inelasticity of particles was considered. However, due to the complexity, most of the earlier theoretical developments of the constitution equations assumed particles smooth and neglected the friction effect. Lun and Savage[6] started to consider the uniform, rough, inelastic spherical particles to study the

Correspondence concerning this article should be addressed to S.-S. Hsiau at sshsiau@cc.ncu.edu.tw.

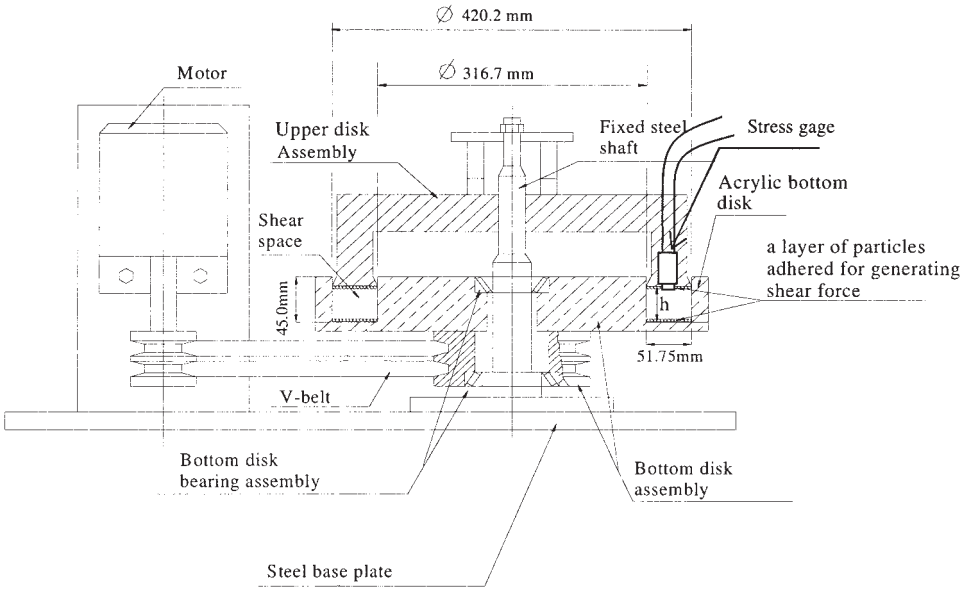


**Figure 1. Experimental apparatus.**

influences of surface friction of particles. In their article, the coefficient of restitution $e_p$ was used to characterize the inelasticity of particles, and the roughness coefficient $\beta$ was adopted to characterize the effects of surface friction and inelasticity in particle collisions. They focused on the high bulk density flow with major contribution of stresses from the collisional mode. Later, Lun[7] considered both the kinetic and the collisional stresses and extended the theory to a system of slightly inelastic and slightly rough spherical particles. In Lun and Bent's numerical simulation[8] of inelastic frictional spheres in a simple shear flow, the results showed that the normal and shear stresses were anisotropic and decreased with the decreasing coefficient of restitution and with the increasing friction coefficient.

There are some experimental works about the sheared granular Couette flows.[9-13] Most of the earlier experiments assumed that the flow generated in the cell was a simple shear flow with constant shear rate and constant granular temperature. However, these assumptions were invalid because of the gravitational force, as demonstrated in the study of Hsiau and Shieh.[14] Hsiau and Yang[15,16] performed a series of tests to measure the transport properties—velocity fluctuations, granular temperatures, and self-diffusion coefficients—and the effective viscosities of sheared granular flows generated in a rotated Couette shear cell. They employed image processing technology to investigate the granular flow behaviors in a shear cell. Instead of using transducers to measure the average stresses, there were three bi-directional stress gages buried in the upper wall to measure the normal and shear stresses of granular materials along the surface. In the past, there were relatively few experimental studies discussing the particle frictional effects due to the limitations of the laboratory. This article tries to experimentally study the effect of the internal friction coefficient of particles on the transport behaviors of the sheared granular flows. Several experiments were performed in a shear cell device rotating in a constant speed using four kinds of granular materials with different friction coefficients. The dependence of the measurements on the friction coefficient will be discussed.

## Experimental Setup

A rotating shear cell was constructed to generate the sheared granular flow, as shown in Figure 1. The shear device consists of a bottom disk and an upper disk. The bottom disk, with outside diameter of 45.00 cm, is driven by a 3 hp AC motor. The rotation speed is controlled by a variable speed inverter and can be measured by a tachometer. The bottom disk is made of plexiglass for observation. An annular trough (inside diameter: 31.67 cm; outside diameter: 42.02 cm; depth: 4.5 cm) was cut in the bottom disk. The stationary upper disk could be inserted into the trough where the granular materials were put in the test section. The test section height $h$ could be adjusted and measured by a dial indicator.

In this study, we used four kinds of beads—glass beads (GB), plastic beads (PB), rubber beads (RB), and silicone beads (SB)—as granular materials in the experiments. All these beads (colors of black and white) have the same average diameter $d_p$ of 3 mm. In the experiments, the white particles served as tracer particles. There were about 5% white particles mixed uniformly with 95% black particles. The average solid fraction of each test was calculated from the total particle mass in the test section divided by the particle density and the test section volume. In this study, five different average solid fractions $\nu$ of 0.62, 0.57, 0.52, 0.47, and 0.42 were used. In order to generate enough shears in the flow, a layer of 3 mm glass beads was adhered to both the bottom and top surfaces, in a random packing organization.

In this study, a simple experimental setup was used to measure the normal restitution coefficient of particles, as shown in Figure 2. Particle 1 on the top of the channel was released freely and moved along a very smooth channel to collide with Particle 2 placed on the bottom of the channel. The particles' velocities before and after collision could be deter-

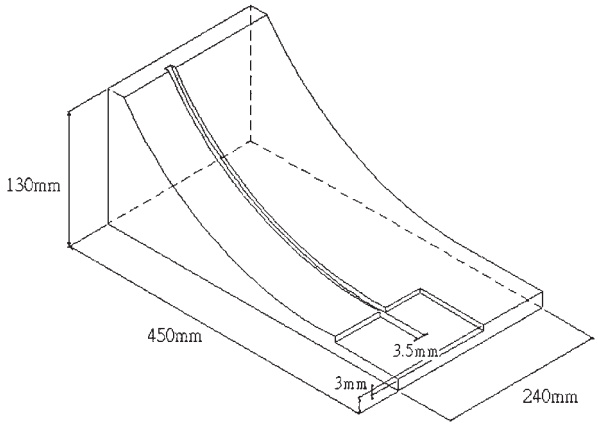


**Figure 2. Experiment setup for measuring the normal restitution coefficient.**

mined by using a high-speed camera. The normal restitution coefficient is defined as:

$$e_p = \frac{V_2' - V_1'}{V_1 - V_2} \tag{1}$$

where $V_1$ and $V_2$ are the velocities of Particles 1 and 2 before collision, and $V_1'$ and $V_2'$ are the corresponding velocities after collision. Note that the coefficient of restitution is generally a function of the magnitude of impact velocity before collision, $|V_1 - V_2|$. In our simple experiments, Particle 2 was stationary before collision ($V_2 = 0$) so that the impact velocity was $V_1$. The mean coefficients of normal restitution were measured from tests with a range of particle impact velocities. In the later experiments performed in a rotating shear cell, the variation of particle impact velocities was not very large for each material. Thus, the variations of $e_p$ for each material due to different impact velocities were neglected. In addition, the internal friction coefficients and wall friction coefficients are measured by a commercial Jenike Shear Tester. The particle densities $\rho_p$, mean coefficients of normal restitution $e_p$, internal friction coefficients $\mu_p$, and wall friction coefficients $\mu_w$ of the four granular materials are listed in Table 1.

Three bi-directional stress gages were installed along the upper wall to measure the normal and shear stresses, as shown in Figure 1. The detecting surfaces of the stress gages are in the same plane with the upper wall surface. The stress gage is based on a simple ring dynamometric element, which is provided with semiconductor strain gages.[17] The normal and shear stresses are realized by two different wiring systems of the strain gages, and the normal and shear stresses can be measured simultaneously. The stress gage utilizes two different full bridge semiconductor strain circuits to measure both stress components simultaneously and independently. The diameter of the measuring surface of the gage is 2.0 cm. The measuring surface can be replaced with the same wall material as the upper surface of the test section. A stable voltage of 10 volts is supplied to each stress gage by a DC power supply. When the stress gages sense the normal and shear forces from the granular materials, the voltage signals are translated from the gages to a personal computer through a data acquisition card (Advantech PCL-818HG). A series of calibration tests were carefully done along two directions. The accuracy of the stress gages is over 99%. The normal and shear stresses are determined from the average signals obtained from the three stress gages.

The granular flow in the test section is assumed to be two-dimensional, with the streamwise (horizontal) direction as the $x$-axis and the transverse (vertical) direction as the $y$-axis (upwards is positive). Because of the limitations on observation, only the flows adjacent to the outer surface of the annular trough in the bottom disk could be recorded and analyzed. The inner surface was cleaned and polished before each experiment to reduce the wall friction effect. The velocity at the bottom (outside lower corner of the trough) $u_0$ could be calculated from the product of the rotational speed of the bottom disk and the outside radius of the trough.

A high-speed camera was used to record the motions of the granular materials. Using image processing technology and the particle tracking method, the average and fluctuation velocities in the streamwise and transverse directions could be measured. In this study, the images were grabbed at a speed of 500 frames per second. The autocorrelation technique was employed to process the stored images and to decide the shift of each tracer particle in every two consecutive images. The details of the autocorrelation process can be found in Hsiau and Shieh.[14]

The test section was also divided into 10 regions along the transverse direction in the experiment of fluctuation velocity. By averaging about 250 tracer particles' velocities from approximately 8500 frames, the overall average velocities in the horizontal and vertical directions, $<u>$ and $<v>$, in each region were determined. The fluctuation velocities in the two directions, $<u'^2>^{1/2}$ and $<v'^2>^{1/2}$, for each region were defined by the mean square root of the deviations of each local velocity from the overall average velocity. The granular temperature $T$ was used to quantify the kinetic energy of the flow, and could be calculated from the average of the mean square of the fluctuation velocities in two directions. Since the current study followed the auto-correlation technique developed by Hsiau and Shieh,[14] which considered the correlation values of gray level derivatives, the experimental errors of the velocities were reduced to within 1.5%.

The velocity fluctuations induce the self-diffusion in granular shear flows. Einstein[18] first employed this concept to analyze the diffusive phenomena of suspended particles with Brownian motion in a liquid. This idea was also used by Savage and Dai[19] and by Campbell[20] to investigate the diffusive behavior of granular flow systems through computer simulation. The self-diffusion coefficient $D_{ij}$ was defined as:

$$\lim_{t\to\infty}\langle \Delta x_i \Delta x_j \rangle = 2D_{ij}t \tag{2}$$

where $\Delta x_i$ and $\Delta x_j$ were the diffusive displacements in directions $i$ and $j$. By tracking enough numbers of particles in a

**Table 1. The Properties of Four Kinds of Particles**

| | Glass Beads (GB) | Plastic Beads (PB) | Rubber Beads (RB) | Silicone Beads (SB) |
|---|---|---|---|---|
| Particle density $\rho_p$ (kg/m$^3$) | 2476 | 1420 | 1415 | 1768 |
| Normal restitution coefficient $e_p$ | 0.96 | 0.95 | 0.94 | 0.92 |
| Internal friction coefficient $\mu_p$ | 0.62 | 0.69 | 0.75 | 0.80 |
| Wall friction coefficient $\mu_w$ | 0.42 | 0.45 | 0.47 | 0.50 |

channel, the self diffusion coefficients could be determined from Eq. 2. Since the distance of the view window of the CCD was relatively short, in order to obtain longer histories of particle movements in a Couette device through a small camera window, the idea of "periodic cell" used in computer simulation[21] was proposed for application in diffusion measurement experiments by Hsiau and Shieh.[14] When a tracer particle moved out of one image, the time counter for this particle was paused. The computer program would then search the following images, until the other tracer was found in the inlet with the same channel height and the same velocities as the former tracer. The path of this new tracer particle from the image inlet was then treated as the continuous movements of the former tracer particle. Since the inlet particle positions were not set by the computer program as in simulation, thousands of images might be needed to get a replaced tracer particle in the inlet with the same velocities and vertical position as the former tracer particle. In the current experiment, the mean-square diffusive displacements $<\Delta x \cdot \Delta x>$ and $<\Delta y \cdot \Delta y>$ were averaged from about 250 tracer particles taken from 2000-4000 frames. The errors of self-diffusion coefficients were estimated within 5%.

## Results and Discussion

We performed five tests for each material, with different average solid fractions $\nu$ of 0.62, 0.57, 0.52, 0.47, and 0.42. The channel height $h$ was fixed as 2.0 cm. The lower wall velocity $u_0$ was set at 1.10 m/s. As mentioned earlier, four different materials with different internal friction coefficients were used: $\mu_p = 0.62$ (glass bead, GB), 0.69 (plastic bead, PB), 0.75 (rubber bead, RB), and 0.80 (silicone bead, SB). As listed in Table 1, the wall friction coefficients $\mu_w$ of these four kinds of beads range from 0.42 to 0.50 and the normal restitution coefficients $e_p$ range from 0.92 to 0.96. The deviations of $\mu_w$ ($\pm 0.04$) and $e_p$ ($\pm 0.02$) between these beads were relatively small compared with the difference in the internal friction coefficients $\mu_p$ ($\pm 0.09$). Thus, we attributed the difference of the measurement results of the four different materials mostly to the difference of internal friction coefficients $\mu_p$.

Figure 3a shows the distributions of the average ensemble velocities in the streamwise and transverse directions, $<u>$ and $<v>$, with solid fraction of 0.52 for the materials with different internal friction coefficients. The transverse velocities are close to 0 because there is no vertical bulk motion in the channel. The streamwise velocity decreases with the height. The flow with smoother particles (lower $\mu_p$) has greater streamwise velocity. Slip velocities exist at the lower and upper walls. The upper slip velocities are about 58-73% of the lower wall velocities. Due to the gravity effect, there exists a "solid-like region"[22] in the lower half of the channel with faster and more uniform velocities in the streamwise direction. The shear rate is higher in the upper section, which is called the "fluid-like region"[22] or "shear layer."[23] From Figure 3a, the values of the shear rates in this region deviated significantly among those cases with different internal friction coefficients. The shear rate is greater for the material with smaller internal friction coefficient $\mu_p$.

The distributions of the fluctuation velocities in both directions for the four materials are shown in Figure 3b. The fluctuations were highly anisotropic, with the much greater

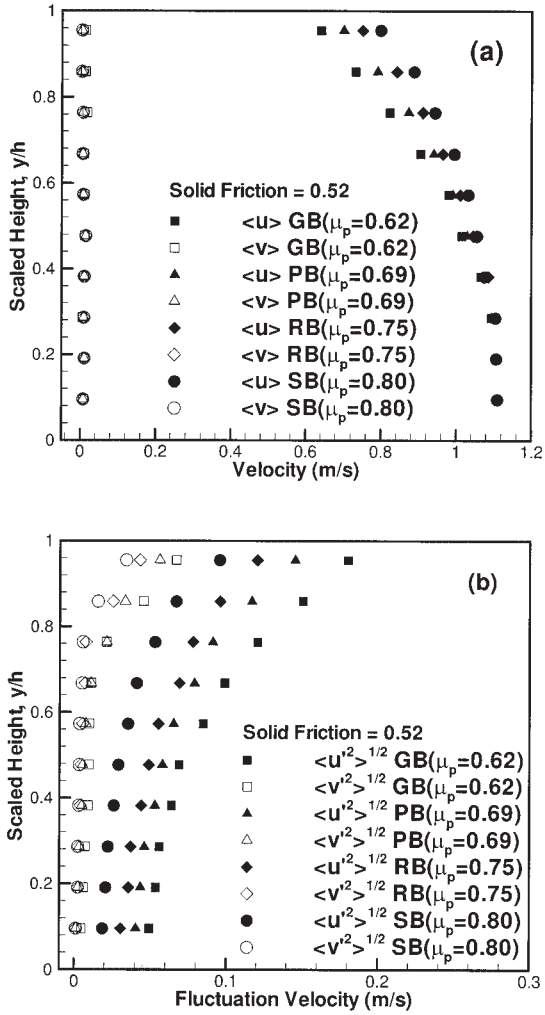


**Figure 3. (a) The ensemble velocity distributions and (b) the fluctuation velocity distributions in the shear cell for four internal friction coefficients cases.**

component in the streamwise direction. The distributions of fluctuations are not isotropic as assumed in the dense-gas kinetic theory.[1] Due to the increasing shear rate ($d<u>/dy$) with the height, the fluctuations also increase with the channel height, as shown in Figure 3b. In addition, the influence of the internal friction coefficient on the fluctuations is significant. The streamwise and transverse fluctuation velocities along the upper wall with internal friction coefficient of 0.62 (GB) are over two times those with internal friction coefficient of 0.80 (SB). Due to particle collisions, there is higher energy dissipated from the granular system with greater friction coefficient $\mu_p$, which causes the smaller fluctuations and shear rates for the higher frictional system.

Figures 4a and b show the dimensionless normal stress $\tau_{yy}/\rho_p d_p^2 (d<u>/dy)^2$ and shear stress $\tau_{xy}/\rho_p d_p^2 (d<u>/dy)^2$ on the upper wall plotted against the solid fraction for the four materials. These two dimensionless stresses were also used in the study of Lun.[7] The shear rates ($d<u>/dy$) were extracted from the streamwise velocity values from the two locations

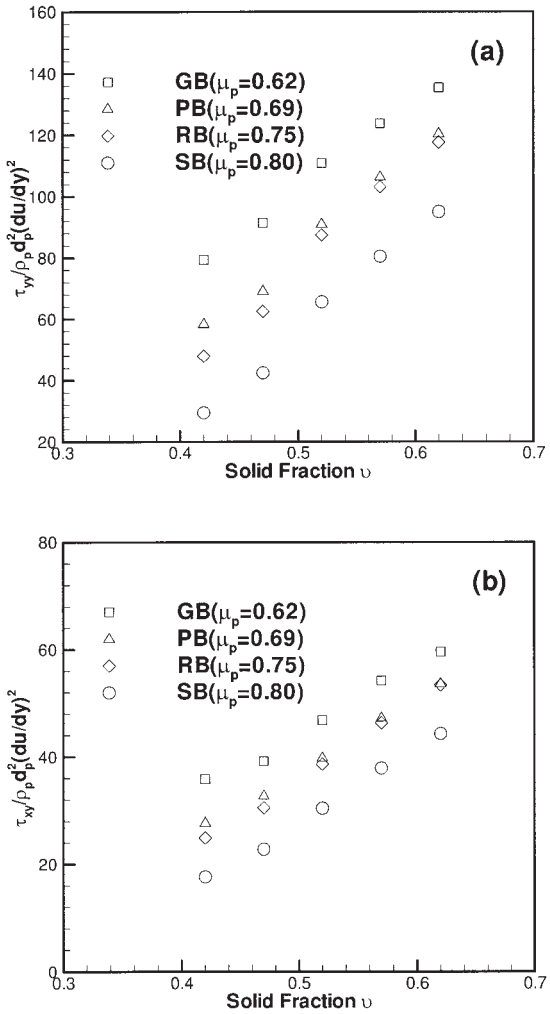


**Figure 4. The dimensionless (a) normal and (b) shear stresses as functions of the solid friction.**

closest to the upper wall from Figure 3a. From dimensional analysis, the normal and shear stresses have the relation of[24]:

$$\tau = \rho_p f(\nu) d_p^2 \left( \frac{d\langle u \rangle}{dy} \right)^2 \tag{3}$$

where $\tau$ is the stress and $f$ is a monotonous increasing function of the solid fraction. In Figures 4a and b, the increase of the dimensionless stresses with the solid fraction is similar to Eq. 3. The similar results were also confirmed by several later experimental studies of dry granular flows.[9-11,16,25] Many simulation works also demonstrated the above relation.[5,21,26-28] In fact, most earlier experimental works used the measured normal and shear forces on the shear cell to calculate the average stresses. Hsiau and Yang[15,16] started to use bi-directional stress gages to measure the local stresses (along the upper wall). The current study used the same instruments to measure the normal and shear stresses. Hsiau and Yang[16] have experimentally studied the effects of solid fractions on the stresses, so we do not intend to discuss this issue here.

In fact, Eq. 3 is applied to the inertially driven granular flows without taking the friction effect into account. Comparing the values of stresses for four different materials from Figures 4a and b, the dimensionless normal and shear stresses are larger for the system with smoother granular materials (lower $\mu_p$). As mentioned earlier, the energy dissipation is higher for the more frictional materials (higher $\mu_p$) during particle collisions, causing higher removal of the particle kinetic energy. Therefore, the normal and shear stresses are lower for the more frictional system.

The results of Figures 4a and b are also consistent with the theoretical development by Lun,[7] who studied four kinds of granular flows with different roughness coefficient in the tangential direction, $\beta$, by using dense-gas kinetic theory. The roughness coefficient depends on the tangential inelasticity, particle surface friction, and impact velocity. In general, $-1 \leq \beta \leq 1$, and $\beta = -1$ denotes perfectly smooth particles and $\beta = 1$ represents particles perfectly elastic and rough. He analyzed the granular materials with different values of $\beta$: $\beta = -1$, $\beta = -0.8$, $\beta = -0.5$, and $\beta = 0$. For $\beta = -1$, since the particles are perfectly smooth, the fluctuation energy is only in the translational mode. The frictional dissipation and the energy exchange between the rotational and translational modes increases with increasing $\beta$. Generally, the larger value of $\beta$ indicates the larger value of $\mu_p$. Lun and Bent[8] also analyzed the effect of particle friction through the discrete element method. Jenkins and Zhang[29] employed kinetic theory to analyze the granular flows with frictional and nearly elastic spheres. Both studies also indicate the similar results that the dimensionless stresses decrease with increasing $\beta$ and $\mu_p$.

Figure 5 shows the ratios of the shear stress to normal stress. The ratio is smaller for the smoother particle system (lower $\mu_p$). But the discrepancy gets smaller for the denser system. The figure also indicates that the stress ratios decrease with the increasing solid fraction when the solid fraction is smaller than 0.5. For solid fractions greater than 0.5, the stress ratio remains close to the value of 0.46, which is the wall friction coefficients $\mu_w$ of the test materials measured by the Jenike Shear Tester. The results are consistent with Hsiau and Yang's[15] conclusion. Since the friction coefficient measured from the Jenike Shear

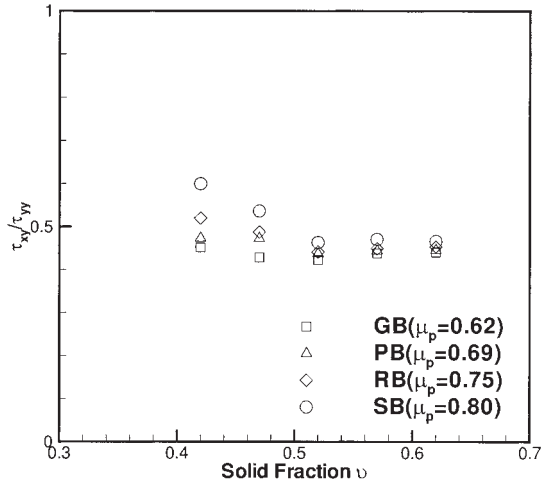


**Figure 5. The ratio of the shear stress to normal stress as functions of the solid fraction.**

Tester is under a relatively dense system, the stress ratio for the lower $\nu$ is different from the wall friction coefficients.

The sheared flow in the current apparatus has different shear rates depending on the location of the channel height $y$ (see Figure 3a). The shear rate is very small in the lower channel, while the shear rate is larger in the upper channel. For the diffusion measurements, the channel is divided into three regions according to the ratio of streamwise velocity to the bottom disk velocity.[1] "Uniform region" is defined for the region with streamwise velocity greater than 95% of the bottom disk velocity. In this region, there is almost no shear.[2] "Low shear region" is the region with the streamwise velocity between 85% and 95% of the bottom disk velocity.[3] "High shear region" is the region with streamwise velocity lower than 85% of the bottom disk velocity. The three flow regimes could be assumed as simple shear flows with constant shear rates.

From the tracked images and the idea of periodic cell, the measured mean-square diffusive displacements in streamwise and transverse directions of the granular material flow of glass beads with solid fraction of 0.52 were plotted against time in Figures 6a and b. The figures demonstrate the linear relation in Eq. 2. The self-diffusion coefficient can be determined from the relation between mean-square diffusive displacements and time, as shown in Eq. 2. For the four different materials with different internal friction coefficients and with solid fraction of 0.52, the self-diffusion coefficients in the streamwise direction, $D_{xx,}$ and in the transverse direction, $D_{yy,}$ in the three flow regimes were plotted against the channel height in Figures 7a and b. The self-diffusion coefficients in the streamwise direction are greater than those in the transverse direction. The diffusion coefficients are greater in the high shear region due the higher shear rate and fluctuations. The diffusion coefficients indicate the disturbed status in the flow field. The smaller diffusion coefficient indicates that the fluid in the flow field is less active. From Figures 7a and b, the system with larger internal friction coefficients (rougher particles) has the smaller diffusion coefficients in the flow field, although the deviation is not significant in the uniform region for the four granular materials. It is consistent with our former discussion and verifies that in a granular flow system, the rougher particles system (larger $\mu_p$) has the higher energy dissipation, causing flow behavior less active and less diffusive where the shear rate, the fluctuations, and the diffusion are relatively lower.

Lun and Savage[6] applied the kinetic theory to a system of inelastic, rough spherical particles to study the effect of particle surface friction and rotary inertia. When the particles are perfectly rough, there is equipartition of fluctuation kinetic energy between the rotary and translatory modes. Lun[7] indicated that the translatory inertia was lower for the rougher particles, but the rotary inertia and the energy dissipation were higher. Due to the difficulty and limitation of experimental technique, this article only measured the movements of particles in the translatory mode; therefore, the diffusion coefficients $D_{xx}$ and $D_{yy}$ calculated from the diffusive displacements, only considered the translational inertia. The sum of the translational energy, the rotary energy, and the energy dissipation is a constant. Thus, the translational inertia increases with the decrease of the rotary inertia and the energy dissipation. From Figures 7a and b, $D_{xx}$ and $D_{yy}$ decrease with the increase of the internal friction coefficient of the materials. It indicates the translational inertia also decreases with the increasing $\mu_p$. Therefore, the rotary

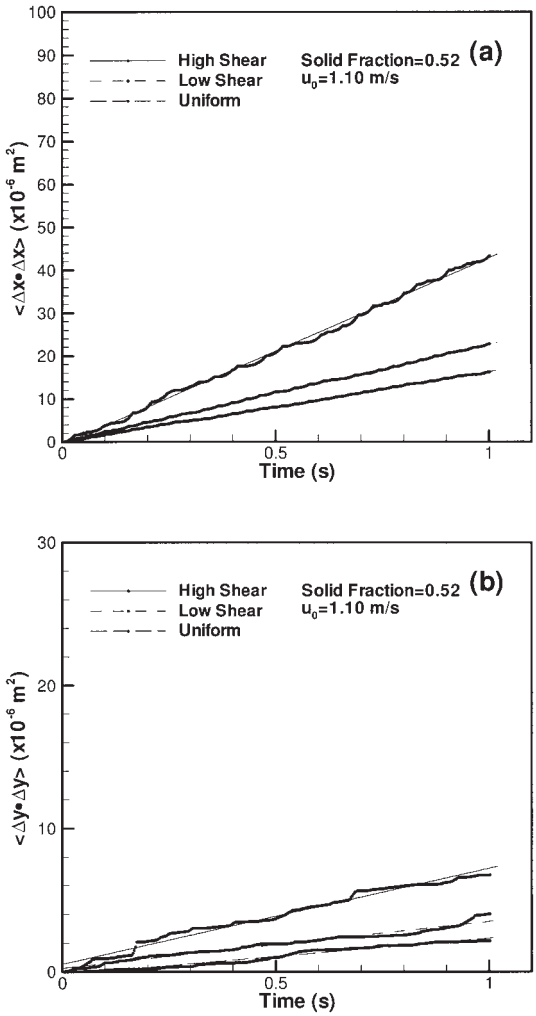


**Figure 6. The mean-square (a) streamwise and (b) transverse displacements varied with time in three flow regions for the internal friction coefficient at 0.62 ($\mu_p$ = 0.62 (GB)).**

inertia and the energy dissipation increase with the increasing $\mu_p$. This experimental indication agrees to the results of Lun and Savage[6] and Lun.[7]

Figures 8a and b show the self-diffusion coefficients in the streamwise and transverse directions in high shear regions versus the solid fraction for the four materials. The influences of the internal friction coefficients on $D_{xx}$ and $D_{yy}$ for the four different materials are similar. From the figures, the diffusion coefficients $D_{xx}$ and $D_{yy}$ increase with decreasing solid fraction. The current experimental results show the similar trend as the theoretical relation between the diffusion coefficient and the solid fraction from the dense-gas kinetic theory[19,30]:

$$D = \frac{d_0\sqrt{\pi T}}{8(1+e_p)\nu g_0(\nu)} \tag{4}$$

where $T$ is the granular temperature and $g_0(\nu)$ is the Carnahan–Starling[31] expression for the radial distribution function at particle contact $g_0(\nu) = (2-\nu)/(2(1-\nu)^3)$. However, the

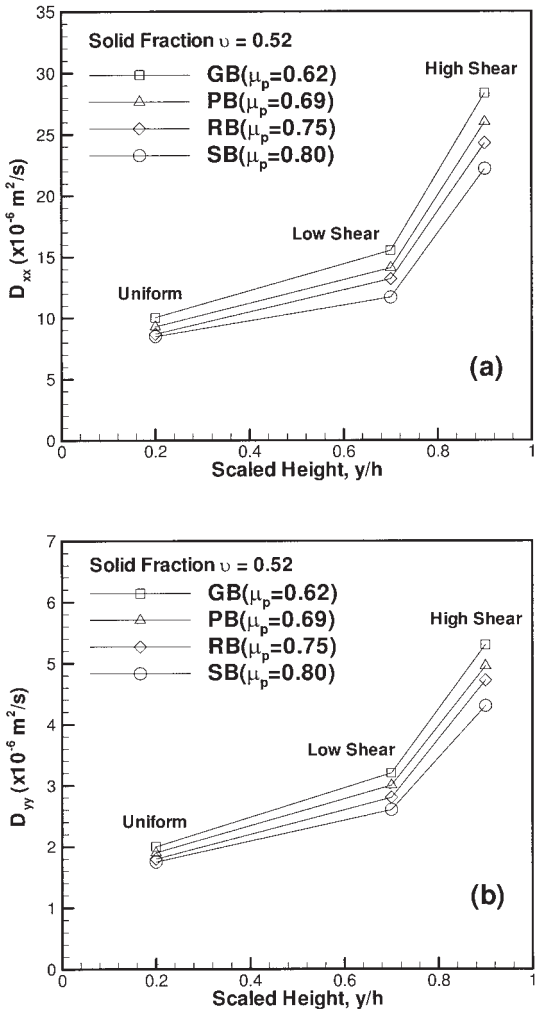


**Figure 7. The self-diffusion coefficients (a) in the streamwise direction and (b) in the transverse direction at the three flow regions versus the channel height for four tests with internal friction coefficients.**

theoretical values of the self-diffusion coefficient are much smaller than the experimental results.[30] The deviation is up to an order of 2 to 3. The significant deviations mainly result from the assumptions in the dense-gas kinetic theory: the isotropic and binary collisions, the isotropic fluctuations, and granular temperature. The relative discussions can be found from our earlier study.[16] It is interesting to note that the influence of $\mu_p$ on diffusion coefficients is more significant in the granular flow with lower solid fraction. From Eq. 4, the diffusion coefficient is inverse to $\nu g_0(\nu)$ and proportional to the square root of $T$. However, for a granular flow with greater solid fraction, the magnitude of $g_0(\nu)$ increased drastically. Therefore, the influence of solid fraction on the diffusion coefficient is much more significant than that of internal friction in the granular flow with higher solid fraction.

## Conclusions

This article studied the effect of particle internal friction on transport behaviors of rough granular material flows in a quasi two-dimensional Couette shear device. The image processing technology and particle tracking method were employed to measure the ensemble velocity, the fluctuation velocities, and the self-diffusion coefficients. Four materials with different internal friction coefficient ($\mu_p$ = 0.62, 0.69, 0.78, and 0.80) were tested.

The effects of internal friction coefficients of particles on transport properties of sheared granular flows were experimentally studied in this work. The shear rates and fluctuation velocities were found to increase with the decreasing internal friction coefficient. The high velocity fluctuations induce the greater self-diffusion coefficients in the high shear region (upper channel). The granular flow with rougher particles has higher energy dissipation, resulting in the lower fluctuations, the lower shear rates, and the smaller self-diffusion coefficient in the test section. The granular flow with smoother particles has the greater dimensionless normal and shear stresses. Also, the granular flow with lower solid fraction has larger discrepancy in diffusion coefficients for the different $\mu_p$ systems.

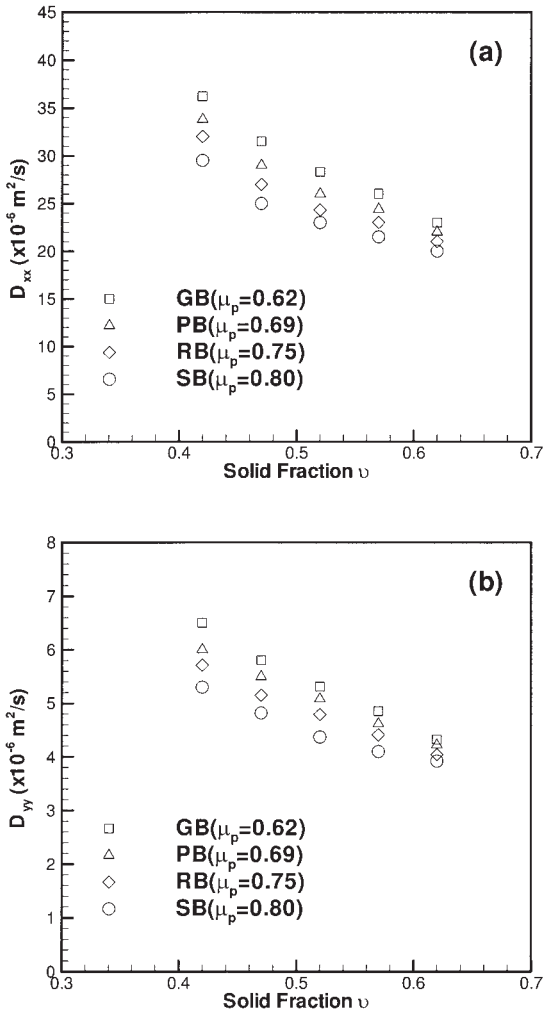


**Figure 8. The self-diffusion coefficients (a) in the streamwise direction and (b) in the transverse direction at the high shear regions versus the solid fraction for 20 tests.**

## Acknowledgments

Financial support from the National Science Council of the R.O.C. (grant NSC 93–2212-E-008–002) is gratefully acknowledged.

## Literature Cited

1. Campbell CS. Rapid granular flows. *Annu Rev Fluid Mech.* 1990;22:57-92.
2. Savage SB, Jeffrey DJ. The stress tensor in a granular flow at high shear rates. *J Fluid Mech.* 1981;110:255-272.
3. Jenkins JT, Savage SB. A theory for the rapid flow of identical, smooth, nearly elastic, particles. *J Fluid Mech.* 1983;130:187-202.
4. Lun CKK, Savage SB, Jeffrey DJ, Chepurniy N. Kinetic theories for granular flow: inelastic particles in Couette flow and slightly inelastic particles in a general flow field. *J Fluid Mech.* 1984;140:223-256.
5. Campbell CS. The stress tensor for simple shear flow of a granular material. *J Fluid Mech.* 1989;203:449-473.
6. Lun CKK, Savage SB. A simple kinetic theory for granular flow of rough, inelastic, spherical particles. *Trans ASME J Appl Mech.* 1987;54:47-53.
7. Lun CKK. Kinetic theory for granular flow of dense, slightly inelastic, slightly rough spheres. *J Fluid Mech.* 1991;258:335-353.
8. Lun CKK, Bent AA. Numerical simulation of inelastic frictional spheres in simple shear flow. *J Fluid Mech.* 1994;233:539-559.
9. Savage SB, Mckeown S. Shear stress developed during rapid shear of dense concentrations of large spherical particles between concentric cylinders. *J Fluid Mech.* 1983;127:453-472.
10. Savage SB, Sayed M. Stresses developed by dry cohesionless granular materials sheared in an annular shear cell. *J Fluid Mech.* 1984;142:391-430.
11. Hanes DM, Inman DL. Observations of rapid flowing granular-fluid flow. *J Fluid Mech.* 1985;150:357-380.
12. Johnson PC, Jackson R. Frictional-collisional constitutive relations for granular materials, with application to plane shearing. *J Fluid Mech.* 1987;176:67-93.
13. Wang DG, Campbell CS. Reynolds analogy for a shearing granular materials. *J Fluid Mech.* 1992;244:527-546.
14. Hsiau SS, Shieh YH. Fluctuations and self-diffusion of sheared granular material flows. *J Rheol.* 1999;43:1049-1066.
15. Hsiau SS, Yang WL. Stresses and transport phenomena in sheared granular flows. *Phys Fluids.* 2002;14:612-621.
16. Hsiau SS, Yang WL. Transport property measurements in sheared granular flows. *Chem Eng Sci.* 2005;60:187-199.
17. Smid J. Pressure gage for measurements of normal and tangential stresses in granular materials. *CZ Patent.* 1980;213:844.
18. Einstein A. *Investigations on the Theory of the Brownian Movement*. (ed. R Furth). New York: Dover Publications Inc; 1956.
19. Savage SB, Dai R. Studies of shear flows. Wall slip velocity, 'Layering' and self-diffusion. *Mechanics of Materials.* 1993;16:225-238.
20. Campbell CS. Self-diffusion in granular shear flows. *J Fluid Mech.* 1997;348:85-101.
21. Campbell CS, Brennen CE. Computer simulation of granular shear flows. *J Fluid Mech.* 1985;151:167-188.
22. Zhang Y, Campbell CS. The interface between fluid-like and solid-like behaviour in two-dimensional granular flows. *J Fluid Mech.* 1992;237:541-568.
23. Aidanpää JO, Shen HH, Gupta RB. Experimental and numerical studies of shear layers in granular shear cell. *J Engineering Mech.* 1996;March:187-196.
24. Bagnold RA. Experiments on a gravity-free dispersion of large solid spheres in a Newtonian fluid under shear. *Proc R Soc London Ser A.* 1954;225:49-63.
25. Craig K, Buckholz RH, Domoto G. An experimental study of the rapid flow of dry cohesionless metal powders. *J Appl Mech.* 1986;53:935-942.
26. Campbell CS, Gong A. The stress tensor in a two-dimensional granular shear flow. *J Fluid Mech.* 1986;164:107-125.
27. Walton OR, Braun RL. Stress calculations for assemblies of inelastic spheres in uniform shear. *Acta Mech.* 1986;63:73-86.
28. Hopkins MA, Shen HH. A Monte-Carlo solution for rapidly shearing granular flows based on the kinetic-theory dense gases. *J Fluid Mech.* 1992;244:477-491.
29. Jenkins JT, Zhang C. Kinetic theory for identical, frictional, nearly elastic spheres. *Phys Fluids.* 2002;14:1228-1235.
30. Hsiau SS, Hunt ML. Kinetic theory analysis of flow-induced particle diffusion and thermal conduction in granular material flows. Trans. *ASME C: J Heat Transf.* 1993;155:541-548.
31. Carnahan NF, Starling KE. Equations of state for non-attracting rigid spheres. *J Chem Phys.* 1969;51:635-636.

*Manuscript received July 3, 2005, and revision received July 25, 2006.*